Sādhanā (2024) 49:241
https://doi.org/10.1007/s12046-024-02590-0

3D biomechanical model that can perform dynamic analysis of the upper extremity and L5/S1 joints without the use of force sensor

MİTHAT YANIKÖREN[1,*], SEZCAN YILMAZ[2] and ÖMER GÜNDOĞDU[3]

[1]Mechatronics Programme, Department of Electronics and Automation, Vocational School, Bilecik Şeyh Edebali University, 11100 Bilecik, Türkiye
[2]Department of Mechanical Engineering, Eskişehir Osmangazi University, 26480 Eskişehir, Türkiye
[3]Department of Mechanical Engineering, Atatürk University, 25240 Erzurum, Türkiye
e-mail: mithat.yanikoren@bilecik.edu.tr; sezcanyilmaz@ogu.edu.tr; omergun@atauni.edu.tr

MS received 19 September 2023; revised 27 December 2023; accepted 12 June 2024;
published online 24 August 2024

Abstract. It is not possible to directly measure the reaction forces and moments acting on the joints in the living things without damaging the integrity of the body. L5/S1 joint in the human body have a higher damage potential than other joints. In this study, it is aimed to develop a method that can calculate the net reaction forces and moments acting on the L5/S1 and upper extremity joints by using only kinematic measurement inputs, without the need for force measurement from the points where the feet contact the ground. For this purpose, 3D biomechanical model suitable for human anatomy was created. Kinematic analyzes were performed using the Denavit–Hartenberg (DH) method. Iterative Newton–Euler (NE) method was used for inverse dynamic calculations. The kinematic measurement inputs of joint movements were obtained by the subject in an experimental study involving the lifting task a certain load from the ground and lowering it to a high place. The model was verified by comparing the results obtained using the proposed method with each other and with the literature data.

Keywords. 3D biomechanical modelling; wearable sensors; inertial measurement unit (IMU); manual material handling; lifting tasks.

1. Introduction

One of the most important features that distinguish living things from inanimate object is ability to move, which takes place depending on mechanical principles. Many studies have been made and continue to be done on the movement analysis and modeling of the musculoskeletal system of the living body [1–11]. Today, researchers are active in many areas where human motion analysis is at the forefront, especially the development of interactive video games, computer-aided film production, interactive education systems and virtual reality applications [12–14]. In many of these areas, only kinematic analysis is sufficient to realistically create movements. However, dynamic analysis is needed in addition to kinematic analysis in areas such as ergonomics, sportive activity analysis and detection of movement disorders in humans.

It is very difficult to develop models that fully characterize the physical activities of living things. In particular, how realistically human postures and movements are depicted is an important aspect of biomechanical modelling. Biomechanical studies can be divided into three parts, respectively, from the early period to the present: static analysis, 2D dynamic analysis in the sagittal plane, and 3D dynamic analysis. In the early generation biomechanics studies, static analyses were made by generally evaluating the human body as if it was motionless [15, 16]. In second generation biomechanical models, motion is examined in two-dimensions over its projection on the sagittal plane [17–20]. Thanks to the developed computer software and motion measurement systems, the examination and analysis of human motion in third generation biomechanics studies has been generalized by moving to the third dimension [21–28].

Due to the flexibility of the joint structures of humans, like many living things, their joints can be damaged temporarily or permanently as a result of excessive strain. For this reason, it is very important to know in which movements and at what level the joints are forced. However, in today's conditions, it is not possible to directly measure the reaction forces and moments affecting the joints between the limbs in the human skeletal system without disturbing the integrity of the body. It is possible to calculate net reaction forces and moments using position, velocity and acceleration data that can be measured

*For correspondence

on the limbs. The calculated net reaction forces are among the components of the reaction force acting on the joint. Joint movements are provided by muscles that work continuously in the draw direction and have a substantially smaller moment arm. Therefore, the forces exerted by the muscles are usually considerably larger than the net reaction forces. The contribution of the net reaction forces to the compression and shear forces acting on the joint is quite small compared to the muscle forces. The reaction moment is the most important parameter to verify, as the net reaction moment describes exactly what level of muscle force is needed to perform a movement [25].

Various institutions, agencies, universities and research centers in many countries have determined that musculoskeletal disorders have the highest ratio with 38.2% among physical diseases caused by manual material handling [29, 30]. According to a similar study, it was determined that 34% of musculoskeletal disorders were caused by manual material lifting. It has been determined that 6% of the musculoskeletal disorders caused by manual material lifting actions occur in the arms and shoulders, 8% in the wrists and ankles and knee joints, 10% in the finger joints and 21% in the back region [31]. In the human body, the L5/S1 joint, which connects the lumbar spine to the sacral spine, is the joint with the highest damage potential. A better understanding of the risk factors for this joint can provide important information about the prevention and management of this condition.

In such a study, 3DSSPP (3D Static Strength Estimation Program), one of the rigid body musculoskeletal modeling tools that can be used to determine the net reaction forces and moments in joints, can only perform static analysis without considering inertia effects [32]. Other alternative software, OpenSim [33] and AnyBody [34], can perform dynamic analysis in a wide range of areas from gait analysis to muscle activities. These software, which also take into account muscle activities in kinetic analysis, can also be used to estimate reaction forces in joints. In addition, by measuring the boundary conditions using a force platform from the points where the participants are in contact with the fixed ground and optimization approaches, these software can perform general analysis for all joints, including the joints of the lower extremities.

In human skeleton models used in previous studies [35] and in package programs for calculating the net reaction forces and moments in joints (3DSSPP, OpenSim, AnyBody, etc.), the reference frame is usually positioned on the L5/S1 joint or pelvis [33, 34, 36]. In this case, in order to calculate the net reaction forces and moments in the L5/S1 joint with the methods using only the angular change data in the joints as input, it is necessary to calculate the net reaction forces and moments of each limb, respectively, starting from the most extreme limbs such as the head, hands and feet. Since the feet are in contact with the fixed ground, it is necessary to measure the reaction force from the ground as a boundary condition in the dynamic analysis starting from the feet.

In a study using two different kinematic measurements (optical motion capture (OMC) and wearable inertial motion capture system (IMC)) and two different force measurements (force plates (FPs) and instrumented force shoes (FSs)) [37], the net reaction moment at the L5/S1 joint during manual lifting was estimated with four different computational models. In another study [25] proposed a 3D calculation method that can be used to calculate the net reaction forces and moments that occur in the joints as a result of asymmetric movements. Using data obtained from a 3-D automatic video-based motion recording system and a force platform, the two calculation methods were compared on the net reaction moments at the L5/S1 joint [25]. In a study [38], where 3D forces and moments were measured externally on hands of participants to estimate L5/S1 joint moments during various manual lifting tasks, maximum L5/S1 net reaction moments were obtained by applying an interpolation method combined with a 3D biomechanical model. In a study [39], in which whole body kinematic measurements and force measurement data from their feet were used during manual load lifting, the force effects on the hands of participants were calculated.

This study presents an approach that aims to estimate the net reaction forces and moments acting on the L5/S1 and upper extremity joints by using only kinematic measurement inputs, without the need for force measurement from the points where the feet contact the ground. It is thought that this method, which can be applied systematically for these purposes, will contribute to the literature. In the application where the proposed model will be used, if an action is to be performed that will cause the feet to lose contact with the ground (such as load carrying), the acceleration of the reference frame should be measured relative to a newly created fixed reference frame and applied as a boundary condition input to the kinematic equations. In the case where the boundary condition is determined with acceleration measurement data, this method can be applied without the need for force platform data for all activities using L5/S1 and other methods [21–28] where the net reaction forces and moments at the upper limb joints can be calculated.

2. Material and methods

Ethics committee approval for the acquisition of the data used in this study was obtained from the Ataturk University, Faculty of Medicine Clinical Research Ethics Committee with the decision dated 02/15/2018 and numbered 44 of the 2nd meeting. The subject was informed about the experiment to be conducted and the "Voluntary Consent Form" was signed.

2.1 *Kinematic model*

The human body skeletal system is a structure where individual bones are connected to each other through joints. These joints differ in shape, function and form. The skeletal

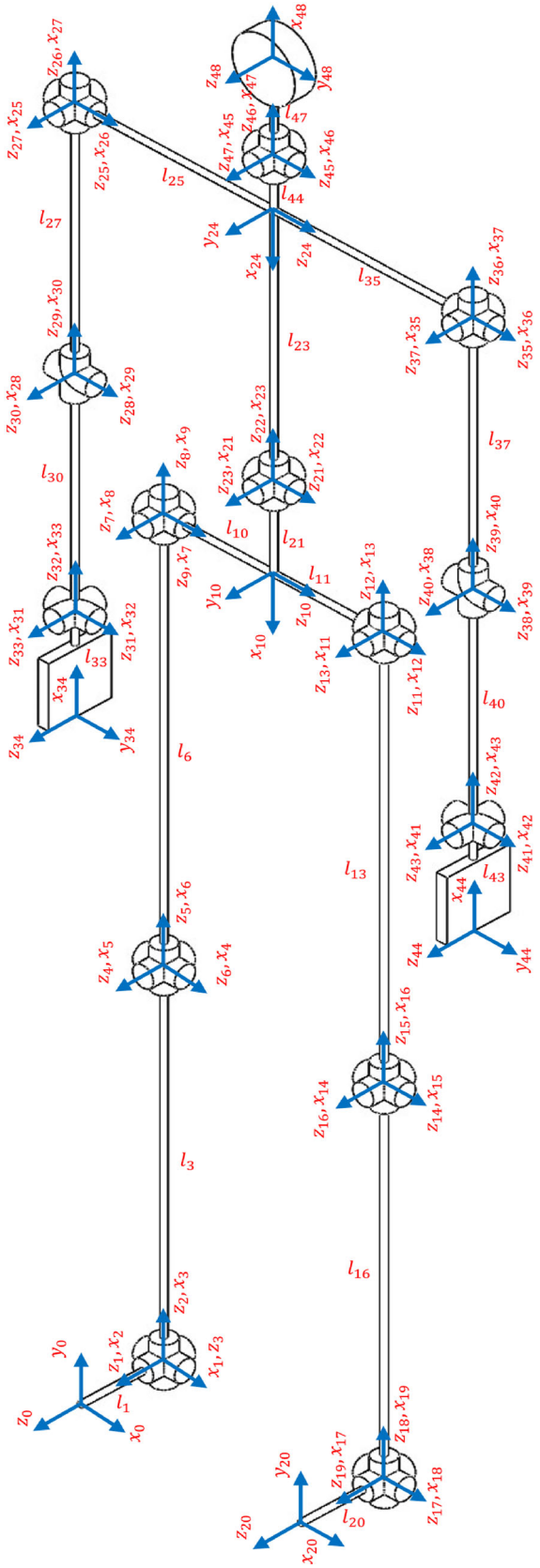

Figure 1. Three-dimensional biomechanical human model (ankles (3 dof), knees (3 dof), hips (3 dof), L5/S1 (3 dof), shoulders (3 dof), elbows (2 dof), wrists (2 dof) ve C4/C5 (3 dof)).

system of the human body can be considered as a three-dimensional mechanical system in which kinematic constraints due to joint movements are taken into account. By adding each bone and joint to the model, it may be possible to model the skeletal system in the best way whichever part of the body is focused on in biomechanical studies, the joints in that area are examined in more detail. For example, in studies on the human spine [27], each vertebra joint is modeled separately and special measurement methods are used. However, in biomechanical studies on the whole body [28, 40], if each bone and joint is represented in the model, the complexity will increase and it is often not possible to accurately determine the movement of each joint from a limited number of measurements. Therefore, when constructing a kinematic model for the skeletal system, it is more appropriate to represent joints (such as those of the vertebral column) with a limited range of motion in the nearest virtual joint within the model. In this study, all of the joint movements between the C1 and C7 vertebrae are represented in the C4/C5 joint. Similarly, all of the joint movements between the T1 and S1 vertebrae are represented in the L5/S1 joint. The present study defines a 3D model, comprised by 15 rigid bodies connected by 14 joints, with a total of 38 degrees of freedom (dof), as shown in figure 1.

The Denavit-Hartenberg (DH) method [41] can be used for kinematic modeling of human movements. This method allows the systematic creation of the translation and rotation relationship between the coordinate axes fixed on the two limbs that are hinged to each other [42]. This systematic approach, which was originally created to reveal the motion relationship between successive limbs in the kinematic chain, has gained popularity especially with its use in serial robot manipulators. The DH method can be used to create a kinematic model of the human skeletal system [43–45]. In the DH method, the frames on a joint between neighbor limbs is created according to a procedure that considers certain constraints [42]. The 49 frames on the kinematic model shown in figure 1 were created by taking this procedure into account. The degree of freedom of each joint was determined in accordance with the anatomical structure of the joint and information about joint movements and frames are given in table 1. In the DH method used in this study to establish kinematic relationships between joints, rotational motion between consecutive frames can only be defined in the z-axis. The z-axis of 38 of the frames are directly related to the freedoms of the physical joints. However, in the DH method, where the rotational freedoms of the physical joints are represented by the z-axis of the frames, it is not always possible to directly define the kinematic constraints [42] between consecutive

Table 1. DH table of the three-dimensional biomechanical model.

Joints	i	α_{i-1} $R_x(z_{i-1} \rightarrow z_i : x_{i-1})$	a_{i-1} $D_x(z_{i-1} \rightarrow z_i : x_{i-1})$	θ_i $R_z(x_{i-1} \rightarrow x_i : z_i)$	d_i $D_z(x_{i-1} \rightarrow x_i : z_i)$
Right leg					
Ankle	1	0	0	θ_1	$-l_1$
	2	$-\pi/2$	0	$\theta_2 - \pi/2$	0
	3	$-\pi/2$	0	$\theta_3 - \pi/2$	0
Knee	4	$-\pi/2$	l_3	$\theta_4 - \pi/2$	0
	5	$-\pi/2$	0	$\theta_5 - \pi/2$	0
	6	$-\pi/2$	0	$\theta_6 - \pi/2$	0
Hip	7	$-\pi/2$	l_6	$\theta_7 - \pi/2$	0
	8	$-\pi/2$	0	$\theta_8 - \pi/2$	0
	9	$-\pi/2$	0	$\theta_9 - \pi/2$	0
Auxiliary frame	10	0	0	π	l_{10}
Left leg					
Hip	11	0	0	$\theta_{11} - \pi/2$	l_{11}
	12	$\pi/2$	0	$\theta_{12} + \pi/2$	0
	13	$\pi/2$	0	$\theta_{13} + \pi/2$	0
Knee	14	$\pi/2$	$-l_{13}$	$\theta_{14} + \pi/2$	0
	15	$\pi/2$	0	$\theta_{15} + \pi/2$	0
	16	$\pi/2$	0	$\theta_{16} + \pi/2$	0
Ankle	17	$\pi/2$	$-l_{16}$	$\theta_{17} + \pi/2$	0
	18	$\pi/2$	0	$\theta_{18} + \pi/2$	0
	19	$\pi/2$	0	$\theta_{19} + \pi/2$	0
Foot	20	0	0	$-\pi/2$	l_{20}
Torso					
L5/S1	21	0	$-l_{21}$	$\theta_{21} - \pi/2$	0
	22	$\pi/2$	0	$\theta_{22} + \pi/2$	0
	23	$\pi/2$	0	$\theta_{23} + \pi/2$	0
Auxiliary frame	24	$\pi/2$	l_{23}	π	0
Right arm					
Shoulder	25	0	0	$\theta_{25} - \pi/2$	$-l_{25}$
	26	$\pi/2$	0	$\theta_{26} + \pi/2$	0
	27	$\pi/2$	0	$\theta_{27} + \pi/2$	0
Elbow	28	$\pi/2$	$-l_{27}$	$\theta_{28} + \pi/2$	0
	29	$\pi/2$	0	$\pi/2$	0
	30	$\pi/2$	0	$\pi/2$	0
Wrist	31	$\pi/2$	$-l_{30}$	$\theta_{31} + \pi/2$	0
	32	$\pi/2$	0	$\theta_{32} + \pi/2$	0
	33	$\pi/2$	0	$\theta_{33} + \pi/2$	0
Hand	34	0	$-l_{33}$	0	0
Left arm					
Shoulder	35	0	0	$\theta_{35} - \pi/2$	l_{35}
	36	$\pi/2$	0	$\theta_{36} + \pi/2$	0
	37	$\pi/2$	0	$\theta_{37} + \pi/2$	0
Elbow	38	$\pi/2$	$-l_{37}$	$\theta_{38} + \pi/2$	0
	39	$\pi/2$	0	$\pi/2$	0
	40	$\pi/2$	0	$\pi/2$	0
Wrist	41	$\pi/2$	$-l_{40}$	$\theta_{41} + \pi/2$	0
	42	$\pi/2$	0	$\theta_{42} + \pi/2$	0
	43	$\pi/2$	0	$\theta_{43} + \pi/2$	0
Hand	44	0	$-l_{43}$	0	0
Head					
Neck (C4/C5)	45	0	$-l_{44}$	$\theta_{45} - \pi/2$	0
	46	$\pi/2$	0	$\theta_{46} + \pi/2$	0
	47	$\pi/2$	0	$\theta_{47} + \pi/2$	0
Head	48	0	l_{47}	0	0

frames. In such cases, auxiliary frames can be used between two consecutive physical joints in order to accurately define the kinematic relationships between them. In the model proposed in this study, the frames {10, 24, 29, 30, 39, 40} are the auxiliary frames used for this purpose. The frames {0, 20, 34, 44, 48} shown in figure 1 are used to indicate the end limbs as right foot, left foot, right hand, left hand and head respectively. Detailed descriptions of the kinematic dimensions of the limbs are given in table 2.

The homogeneous transformation matrix contains rotation and translation data between two frames, one of which is the reference frame. Homogeneous transformation matrix defined between reference frame $\{i-1\}$ and moving frame $\{i\}$,

$$ {}^{i-1}_{i}\boldsymbol{T} = \begin{bmatrix} {}^{i-1}_{i}\boldsymbol{R} & {}^{i-1}\boldsymbol{P}_i \\ 0 & 1 \end{bmatrix} \tag{1} $$

Here ${}^{i-1}_{i}\boldsymbol{R}$ denotes the rotation matrix (3×3), while ${}^{i-1}\boldsymbol{P}_i$ denotes the translation vector (3×1). In order to obtain the homogeneous transformation matrix ${}^{i-1}_{i}\boldsymbol{T}$ with the DH method, a motion set consisting of two rotations $\boldsymbol{R}_x(\alpha_{i-1})$ and $\boldsymbol{R}_z(\theta_i)$ and two translations $\boldsymbol{D}_x(a_{i-1})$ and $\boldsymbol{D}_z(d_i)$ is used in a certain order. In this study, the transformation matrix was obtained as,

$$ {}^{i-1}_{i}\boldsymbol{T} = \boldsymbol{R}_x(\alpha_{i-1})\boldsymbol{D}_x(a_{i-1})\boldsymbol{R}_z(\theta_i)\boldsymbol{D}_z(d_i) \tag{2} $$

In this case, the homogeneous transformation matrix,

$$ {}^{i-1}_{i}\boldsymbol{T} = \begin{bmatrix} \cos\theta_i & -\sin\theta_i & 0 & a_{i-1} \\ \sin\theta_i\cos\alpha_{i-1} & \cos\theta_i\cos\alpha_{i-1} & -\sin\alpha_{i-1} & -d_i\sin\alpha_{i-1} \\ \sin\theta_i\sin\alpha_{i-1} & \cos\theta_i\sin\alpha_{i-1} & \cos\alpha_{i-1} & d_i\cos\alpha_{i-1} \\ 0 & 0 & 0 & 1 \end{bmatrix} \tag{3} $$

Although the DH table method was created for series-connected mechanisms, the human body skeletal system is in a parallel mechanism structure. However, it is possible to express the human skeletal system as a combination of several series of mechanisms. In this context, in the DH table created for the proposed model with 38 DOF, the right foot is taken as a reference point with frame {0}. From the reference frame, serial mechanisms can be created with the sequence of frames {0-10, 21-34} up to the right hand, {0-10, 21-24, 35-44} up to the left hand, {0-10, 21-24, 45-48} up to the head and {0-20} up to the left foot. In line with this information, the DH table given in table 1 was created by considering the kinematic relations between the coordinate systems given in figure 1. Using the DH table and Eq. (3), homogeneous transformation matrices between successive joints can be created. The transformation matrix between each joint of the model is defined sequentially by using local frame. The position and rotation values of the desired joint can be calculated by multiplying these matrices with each other according to the outward kinematic solution method.

2.2 *Dynamics model*

In this study, the net reaction force and moment values on the limbs and joints of the body were calculated according to the iterative Newton–Euler method. In this study, the net reaction force and moment values on the limbs and joints of the body were calculated according to the iterative Newton-Euler method, known as the inverse dynamics approach. This approach allows the indirect calculation of the reaction forces and moments by utilizing the kinematics and inertia properties of bodies in motion. The Newton-Euler method is frequently used in biomechanical calculations because it allows the estimation of the net reaction forces and moments in each joint [25, 46].

In the inverse dynamic approach, first of all, the angular velocity and acceleration of each limb and the linear acceleration of the limb center of mass should be calculated. For this, the speed and acceleration values for each limb are calculated instantly by following the sequence from the reference frame set to the farthest frame [42],

$$ {}^{i+1}\boldsymbol{\omega}_{i+1} = {}^{i+1}_{i}\boldsymbol{R}\ {}^{i}\boldsymbol{\omega}_i + \dot{\theta}_{i+1}\,{}^{i+1}\hat{\boldsymbol{Z}}_{i+1} \tag{4} $$

$$ {}^{i+1}\dot{\omega}_{i+1} = {}^{i+1}_{i}\boldsymbol{R}\ {}^{i}\dot{\omega}_i + {}^{i+1}_{i}\boldsymbol{R}\,{}^{i}\boldsymbol{\omega}_i \times \dot{\theta}_{i+1}\,{}^{i+1}\hat{\boldsymbol{Z}}_{i+1} + \ddot{\theta}_{i+1}\,{}^{i+1}\hat{\boldsymbol{Z}}_{i+1} \tag{5} $$

$$ {}^{i+1}\dot{\boldsymbol{v}}_{i+1} = {}^{i+1}_{i}\boldsymbol{R}\ \left({}^{i}\dot{\omega}_i \times {}^{i}\boldsymbol{P}_{i+1} + {}^{i}\boldsymbol{\omega}_i \times \left({}^{i}\boldsymbol{\omega}_i \times {}^{i}\boldsymbol{P}_{i+1}\right) + {}^{i}\dot{\boldsymbol{v}}_i\right) \tag{6} $$

$$ {}^{i+1}\dot{\boldsymbol{v}}_{c_{i+1}} = {}^{i+1}\dot{\omega}_{i+1} \times {}^{i+1}\boldsymbol{P}_{C_{i+1}} + {}^{i+1}\boldsymbol{\omega}_{i+1} \times \left({}^{i+1}\boldsymbol{\omega}_{i+1} \times {}^{i+1}\boldsymbol{P}_{C_{i+1}}\right) + {}^{i+1}\dot{\boldsymbol{v}}_{i+1} \tag{7} $$

Here vectors ${}^{i}\boldsymbol{\omega}_i$, ${}^{i}\dot{\boldsymbol{\omega}}_i$ and ${}^{i}\dot{\boldsymbol{v}}_i$ represent the projections of the angular velocity, angular acceleration and linear acceleration vectors of the frame number $\{i\}$ on the frame numbered $\{i\}$. The vector ${}^{i+1}\dot{\boldsymbol{v}}_{c_{i+1}}$ expresses the projection of the linear acceleration of the center of mass of the limb containing the frame numbered $\{i+1\}$ on the frame numbered $\{i+1\}$. The vector ${}^{i+1}\boldsymbol{P}_{C_{i+1}}$ represents the position vector of the center of mass of the member containing the frame $\{i+1\}$ with respect to the frame $\{i+1\}$. The ${}^{i+1}_{i}\boldsymbol{R}$ matrix represents the rotation matrix of the frame $\{i\}$ with respect to the frame $\{i+1\}$. The ${}^{i+1}\hat{\boldsymbol{Z}}_{i+1}$ vector is used to represent the active rotation θ_{i+1} axis of the frame $\{i+1\}$. In this study, since the DH tables method is used for kinematic analysis, the frames are designed in such a way that active rotations take place in the z axis. Therefore, ${}^{i+1}\hat{\boldsymbol{Z}}_{i+1} = [0 \quad 0 \quad 1]^{\mathrm{T}}$ is used. Variables $\dot{\theta}_{i+1}$ and $\ddot{\theta}_{i+1}$ are used to express the angular velocity and angular accelerations of the active rotation axis of the frame $\{i+1\}$, respectively.

If the ${}^{MRF}\dot{\boldsymbol{v}}_{MRF}$ linner acceleration of the right foot where frame {0} is located can be measured or derived from the motion capture data, the ${}^{0}\dot{\boldsymbol{v}}_0$ acceleration, which is the initial boundary condition input of Equation (6), can be calculated using the ${}_{MRF}{}^{0}\boldsymbol{R}$ rotation matrix between the

reference frame where the acceleration is measured and frame {0},

$$ {}^{0}\dot{\boldsymbol{v}}_0 = {}^{0}_{MRF}\boldsymbol{R}\ {}^{MRF}\dot{\boldsymbol{v}}_{MRF} \tag{8} $$

Limbs of living things are not rigid objects, and mass and moments of inertia can change over time depending on whether the muscles on them are free or contracted. In this case, in order to obtain the expressions of inertia force ${}^{i+1}\boldsymbol{F}_{i+1}$ and moment ${}^{i+1}\boldsymbol{N}_{i+1}$ acting on each limb, the Newton-Euler equations are,

$$ {}^{i+1}\boldsymbol{F}_{i+1} = m_{i+1}\,{}^{i+1}\dot{\boldsymbol{v}}_{C_{i+1}} + \frac{dm_{i+1}}{dt}\,{}^{i+1}\boldsymbol{v}_{C_{i+1}} \tag{9} $$

$$ \begin{aligned} {}^{i+1}\boldsymbol{N}_{i+1} = {}^{C_{i+1}}\boldsymbol{I}_{i+1}\,{}^{i+1}\dot{\omega}_{C_{i+1}} + {}^{i+1}\boldsymbol{\omega}_{i+1} \times {}^{C_{i+1}}\boldsymbol{I}_{i+1}\,{}^{i+1}\boldsymbol{\omega}_{i+1} \\ + \frac{d^{C_{i+1}}\boldsymbol{I}_{i+1}}{dt}\,{}^{i+1}\boldsymbol{\omega}_{i+1} \end{aligned} \tag{10} $$

can be written as. Here, the variable m_{i+1} represents the mass of the limb containing the frame $\{i+1\}$. The matrix ${}^{C_{i+1}}\boldsymbol{I}_{i+1}$ represents the moment of inertia matrix of the limb containing the frame $\{i+1\}$ with respect to the center of mass. However, although the mass and mass moments of inertia of living limbs are variable, this change is quite small and its effects on the total force are negligible since living limbs cannot move at very high speeds. In this context, there will be no harm in treating living limbs as rigid bodies. In this case, Eqs. (9,10) can be rewritten assuming that the limb mass and mass moment of inertia do not change with time [42],

$$ {}^{i+1}\boldsymbol{F}_{i+1} = m_{i+1}\,{}^{i+1}\dot{\boldsymbol{v}}_{C_{i+1}} \tag{11} $$

$$ {}^{i+1}\boldsymbol{N}_{i+1} = {}^{C_{i+1}}\boldsymbol{I}_{i+1}\,{}^{i+1}\dot{\omega}_{C_{i+1}} + {}^{i+1}\boldsymbol{\omega}_{i+1} \times {}^{C_{i+1}}\boldsymbol{I}_{i+1}\,{}^{i+1}\boldsymbol{\omega}_{i+1} \tag{12} $$

For the inverse dynamic calculation, Equations (4)–(7) and (11), (12) are iteratively solved outward for each frame. In the outward iterations, these equations are respectively, starting from the frame {0} located at the right foot; It is operated with {0-10} frame sets to pelvis, {10, 11-20} frame sets to left foot, {10, 21-24} frame sets to neck, {24, 25-34} frame sets to right hand, {24, 35-44} frame sets to left hand and {24, 45-48} frame sets to head. In this way, the inertia forces and moments belonging to the limbs are obtained.

In order to calculate the net reaction force and moment values acting on the joints, an inward iterative calculation should be made for each limb by following the sequence starting from the farthest frame to the base frame. By using the forces and moments of inertia, the net reaction force ${}^{i}\boldsymbol{f}_i$ and moment ${}^{i}\boldsymbol{n}_i$ values acting on the joints can be calculated [42],

$$ {}^{i}\boldsymbol{f}_i = {}^{i}\boldsymbol{F}_i + {}^{i}_{i+1}\boldsymbol{R}^{i+1}\boldsymbol{f}_{i+1} \tag{13} $$

$$ {}^{i}\boldsymbol{n}_i = {}^{i}\boldsymbol{N}_i + {}^{i}\boldsymbol{P}_{C_i} \times {}^{i}\boldsymbol{F}_i + {}^{i}_{i+1}\boldsymbol{R}^{i+1}\boldsymbol{n}_{i+1} + {}^{i}\boldsymbol{P}_{i+1} \times {}^{i}_{i+1}\boldsymbol{R}^{i+1}\boldsymbol{f}_{i+1} \tag{14} $$

As can be seen in the kinematic diagram of the human skeleton given in figure 1, there are multiple endpoints in the frame {20, 34, 44, 48} in the proposed model. Equations (13), (14) are used for inward iterative calculation in inverse dynamic analysis. These equations are run iteratively inward on the frames of model, {34-25} for the right arm, {44-35} for the left arm and {48-45} for the head, respectively. The net reaction force and moment effects from the right arm, left arm and head are combined in the frame {24},

$$ {}^{24}\boldsymbol{f}_{24} = {}^{24}\boldsymbol{F}_{24} + {}^{24}_{25}\boldsymbol{R}^{25}\boldsymbol{f}_{25} + {}^{24}_{35}\boldsymbol{R}^{35}\boldsymbol{f}_{35} + {}^{24}_{45}\boldsymbol{R}^{45}\boldsymbol{f}_{45} \tag{15} $$

$$ \begin{aligned} {}^{24}\boldsymbol{n}_{24} = {}^{24}\boldsymbol{N}_{24} + {}^{24}\boldsymbol{P}_{C_{24}} \times {}^{24}\boldsymbol{F}_{24} + {}^{24}_{24}\boldsymbol{R}^{25}\boldsymbol{n}_{25} \\ + {}^{24}\boldsymbol{P}_{25} \times {}^{24}_{25}\boldsymbol{R}^{25}\boldsymbol{f}_{25} \\ + {}^{24}_{35}\boldsymbol{R}^{35}\boldsymbol{n}_{35} + {}^{24}\boldsymbol{P}_{35} \times {}^{24}_{35}\boldsymbol{R}^{35}\boldsymbol{f}_{35} + {}^{24}_{45}\boldsymbol{R}^{45}\boldsymbol{n}_{45} \\ + {}^{24}\boldsymbol{P}_{45} \times {}^{24}_{45}\boldsymbol{R}^{45}\boldsymbol{f}_{45} \end{aligned} \tag{16} $$

Then again, using Eqs. (13), (14), the net reaction forces and moments are calculated from the frame {24} to the frame {21}. Thus, the net reaction force and moment values belonging to the L5/S1 joint of the body are obtained according to the frame {21}.

In order to make the proposed method in this paper more understandable, the iteration steps are presented as outward and inward. In outward iterations, i_{ref} is the index of the initial condition of the first element of the operations to be performed for Eqs. (4)–(7), (11), (12) in the corresponding row. Auxiliary frames {10} and {24} are also used for these purposes in the iteration process.

Outward iterations

${}^{i}_{i}\boldsymbol{T} \leftarrow$ Equation (3) for $i : 1 \rightarrow 48$
${}^{i}_{i}\boldsymbol{R}, {}^{i}\boldsymbol{P}_i \leftarrow$ Equation (1) for$i : 1 \rightarrow 48$
${}^{0}\dot{\boldsymbol{v}}_0 \leftarrow$ Equation (8)
${}^{i}\boldsymbol{F}_i, {}^{i}\boldsymbol{N}_i \leftarrow$ Equations $(4-7,11,12)$ for $i_{ref} = 0 \& i : 1 \rightarrow 10$
${}^{i}\boldsymbol{F}_i, {}^{i}\boldsymbol{N}_i \leftarrow$ Equations $(4-7,11,12)$ for $i_{ref} = 10 \& i : 11 \rightarrow 20$
${}^{i}\boldsymbol{F}_i, {}^{i}\boldsymbol{N}_i \leftarrow$ Equations $(4-7,11,12)$ for$i_{ref} = 10 \& i : 21 \rightarrow 24$
${}^{i}\boldsymbol{F}_i, {}^{i}\boldsymbol{N}_i \leftarrow$ Equations $(4-7,11,12)$ for$i_{ref} = 24 \& i : 25 \rightarrow 34$
${}^{i}\boldsymbol{F}_i, {}^{i}\boldsymbol{N}_i \leftarrow$ Equations $(4-7,11,12)$ for$i_{ref} = 24 \& i : 35 \rightarrow 44$
${}^{i}\boldsymbol{F}_i, {}^{i}\boldsymbol{N}_i \leftarrow$ Equations $(4-7,11,12)$ for$i_{ref} = 24 \& i : 45 \rightarrow 48$

Inward iterations

${}^{i}\boldsymbol{f}_i, {}^{i}\boldsymbol{n}_i \leftarrow$ Equations(13,14) for $i : 47 \rightarrow 45$
${}^{i}\boldsymbol{f}_i, {}^{i}\boldsymbol{n}_i \leftarrow$ Equations (13,14) for $i : 43 \rightarrow 35$
${}^{i}\boldsymbol{f}_i, {}^{i}\boldsymbol{n}_i \leftarrow$ Equations (13,14) for $i : 33 \rightarrow 25$
${}^{24}\boldsymbol{f}_{24}, {}^{24}\boldsymbol{n}_{24} \leftarrow$ Equations (15,16)
${}^{i}\boldsymbol{f}_i, {}^{i}\boldsymbol{n}_i \leftarrow$ Equations (13,14) for $i : 23 \rightarrow 21$

2.3 *Instrumentation*

In the biomechanics of human movement, measuring kinematic data forms the basis of other kinematic and kinetic analyzes. Many techniques have been used to collect kinematic data in the literature. Among these techniques that are frequently used in research studies are optoelectronic techniques [9, 25, 46–48], depth sensors and wearable inertial measurement units (IMU) [49–52]. Since optical motion capture systems are not mobile, their use in very narrow or very large spaces is very limited. IMUs allow experimental work in almost any environment and condition thanks to their positioning directly on the person. In this study, wearable IMUs were used to measure joint movements. The IMU is a combined unit that does not measure angular position directly, but includes a 3-axes accelerometer, 3-axes gyroscope and 3-axes magnetometer. Using measurement data from an IMU, it is possible to calculate angular position relative to gravity and magnetic field of the earth reference. By systematically placing more than one IMU on the human body in a certain order, it is possible to calculate the angular positions of certain joints from the data obtained. In this study, STT-IWS (Inertial Wireless Systems) wearable IMUs named by the manufacturer STT Systems with its own name were used. The raw data collected from the IMUs throughout the movement were converted into the angular position data of the joints through the iSenV2020.0 program of the STT Systems.

During the experiments, 16 IMUs (feet (2), lower legs (2), upper legs (2), waist (1), hands (2), lower arms (2), upper arms (2), chest (1), thoracic vertebrae T3 (1) and head (1)) are attached to limbs of subject in a certain order, as seen in figure 2.

2.4 *Data pre-processing*

Movement data of the participants were collected with a sampling frequency of 100 Hz. From studies on parameter selection for the low-pass Butterworth filter used in biomechanical studies [28, 53], the optimum cut-off frequency corresponding to a sampling frequency of 100 Hz is calculated as 6.8 Hz. Cut-off frequency derived from the residual analysis of the optimum cut-off frequency is approximately 5 Hz [53]. This determined cut-off frequency is a recommendation and can be used higher or lower depending on the characteristics of the application. Select a high value of the cut-off frequency will provide a high match between the filtered data and the measured raw data. If a low value of the cut-off frequency is selected, a poor match is observed. However, it should be noted that by selecting a high cut-off frequency will not eliminate low-frequency noise from the raw data [54]. If low-frequency noise is not sufficiently filtered, taking the first and especially the second time derivatives of the filtered data poses challenges [28]. In this study, angular position data was obtained from IMUs. Throughout the movements of subjects, the muscles in the areas where the IMUs are positioned are constantly contracting and relaxing. These contractions and relaxations cause unwanted noise at low frequencies in the raw position data. In this study, angular velocity and acceleration values of the joints were calculated using the forward direction numerical derivative technique from the angular position change data. Angular velocity and acceleration data calculated with the forward direction numerical derivative method are very sensitive to small measurement errors in the angular position. In order to avoid low-frequency noise as much as possible, the cut-off frequency of the sixth-order low-pass Butterworth filter

Figure 2. The experimental setup.

used to filter the angular position data was determined as 2.5 Hz, in line with reference studies [28, 46]. Angular position data of all joints were filtered using a low-pass Butterworth filter.

2.5 *Anthropometric measurements*

In order to calculate the net reaction forces and moments with the proposed method, first of all, raw data of the variation of joint angles θ_i with time are needed. In addition, the kinematic dimensions l_i of the musculoskeletal system of the subject, the masses m_i of the body parts and the mass moment of inertia matrices ${}^{C_i}\boldsymbol{I}_i$ according to the centers of mass are needed. The anthropometric data presented as an example in this section refer to a 36-year-old male participant, 169 cm tall and 84 kg.

Anthropometric studies are carried out in order to determine the length and mass of the limbs, the position of the center of mass and the mass moment of inertia of each limb. In this study, the kinematic dimensions of the subject's body parts (table 2) were determined using the methods in the US Air Force Research Laboratory Reports [55].

In determining the masses of the body parts of the subject, the method based on the assumption of the ratio of body part masses to the total body mass given by Gillette was used [56]. With this method, the body parts masses of the subject are presented in table 3. The load m_L to be lifted is modeled by adding equal masses to both hands masses from the moment it does not touch the ground until it is lowered onto the platform.

In case of motion in free space, the mass moment of inertia of an object that is not perfectly symmetrical will have different values in different directions. In this case, the matrix moment of inertia relative to the center of mass of limb i can be expressed as ${}^{C_i}\boldsymbol{I}_i$,

$$ {}^{C_i}\boldsymbol{I}_i = \begin{bmatrix} I_{xx} & I_{xy} & I_{xz} \\ I_{yx} & I_{yy} & I_{yz} \\ I_{zx} & I_{zy} & I_{zz} \end{bmatrix}_i \tag{17} $$

Here I_{xx}, I_{yy} and I_{zz} represent the mass moments of inertia in the principal axes of inertia. Other terms, $I_{xy}, I_{yx}, I_{xz}, I_{zx}, I_{yz}$ and I_{zy} are called the mass products of inertia. It is possible to calculate the mass moments of inertia needed for the biomechanical model by considering the body parts as simplified geometries. In this study, the

Table 2. Kinematic measurements of body parts.

Kinematic dimensions	Parameter	Length (cm)
Distance from center of heel to big toe	l_1;l_{20}	24
Distance between ankle joint and knee joint	l_3; l_{16}	34
Distance between knee joint and hip joint	l_6;l_{13}	44
Distance between hip joints	$l_{10} + l_{11}$	28
Vertical distance from hip joint to L5/S1 joint	l_{21}	16
Vertical distance between L5/S1 joint and shoulder joint	l_{23}	49
Distance between shoulder joints	$l_{25} + l_{35}$	38
Distance between shoulder joint and elbow joint	l_{27};l_{37}	30
Distance between elbow joint and wrist joint	l_{30};l_{40}	25
Distance between palm and wrist joint	l_{33};l_{43}	10
Vertical distance from shoulder to C4/C5	l_{44}	10
Vertical distance between C1 and C4/C5	l_{47}	8

Table 3. The calculated limb mass/body mass ratio of the subject.

Limb	Symbol	Limb mass/body mass (%)	Subject mass (kg)
Foot	m_1, m_{20}	1.47	1.18
Calf	m_3, m_{16}	4.10	3.28
Thigh	m_6, m_{13}	14.00	11.20
Torso	m_{23}	44.00	35.20
Upper arm	m_{27}, m_{37}	2.70	2.16
Forearm	m_{30}, m_{40}	1.51	1.21
Hand	m_{33}, m_{43}	0.62	0.50
Head	m_{47}	7.20	5.76

Table 4. Mass moments of inertia of limbs relative to their centers of mass.

Limb	Symbol	Mass moments of inertia of limbs (kg.m^2)
Torso	${}^{C_{23}}\boldsymbol{I}_{23}$	$I_{xx} = 0.843;\ I_{yy} = 0.080\ ;\ I_{zz} = 0.833$
Upper arm	${}^{C_{27}}\boldsymbol{I}_{27}, {}^{C_{37}}\boldsymbol{I}_{37}$	$I_{xx} = 0.0062;\ I_{yy} = 0.0173\ ;\ I_{zz} = 0.0165$
Forearm	${}^{C_{30}}\boldsymbol{I}_{30}, {}^{C_{40}}\boldsymbol{I}_{40}$	$I_{xx} = 0.00129;\ I_{yy} = 0.00951\ ;\ I_{zz} = 0.00881$
Head	${}^{C_{47}}\boldsymbol{I}_{47}$	$I_{xx} = 0.0225;\ I_{yy} = 0.0174\ ;\ I_{zz} = 0.0205$
All		$I_{xy} = I_{yx} = I_{xz} = I_{zx} = I_{yz} = I_{zy} = 0$

Table 5. Characteristics of participants (mean ± SD).

	Participants	Age (years)	Weight (kg)	Height (cm)
This study	7 female and 7 male	25.5 ± 5	68 ± 16	170 ± 11
Reference study [37]	8 female and 8 male	32.0 ± 10	69 ± 12	171 ± 9
Reference study [38]	11 male	24.5 ± 4.7	72 ± 9.1	183.3 ± 4.8
Reference study [25]	7 male	31.0 ± 16.9	76.4 ± 5	177 ± 4

mass moment of inertia values was calculated with the formulations of a reference study [56] using anthropometric data measured on the subject. The mass moment of inertia values calculated for the body parts of the subject are given in table 4.

2.6 *Experimental procedures*

Manual material lifting requires complex movements of the musculoskeletal system. For this reason, the analysis of load-lifting action is a very good exemplary application to calculate the net reaction forces and moments that occur in the joints during the movement of the musculoskeletal system. In this study, it is planned to establish an experimental task in parallel with the reference studies [25, 37, 38] in the experimental validation of the proposed model. The characteristics of the participants in this and the reference studies are given in table 5.

In the reference study [37], a 10 kg load was lifted from the ground in different styles and placed on the ground at different distances horizontally. In this context, the subjects were made to perform movements in four different combinations,

1. Free-style lift from a low vertical and a close horizontal position (free-low-close)
2. Free-style lift from a low vertical and a far horizontal position (free-low-far)
3. Asymmetric lift from a low vertical and a close horizontal position (asy-low-close)
4. Free-style from a high vertical and a close horizontal position (free-high-close)

In this study, in parallel with the reference studies [25, 37–39], experimental tasks were established in which the participants would perform lifting a 10 kg load from the ground and relasing it at different horizontal distances in four different styles. These tasks,

1. Lifting the load by squatting from the ground and lowering it symmetrically on the platform at close (squat-symmetric-close).
2. Lifting the load by stoop from the ground and lowering it symmetrically on the platform at far (stoop-symmetric-far).
3. Lifting the load by squatting from the ground and lowering it asymmetrically on the platform at close (squat-asymmetric-close).
4. Lifting the load by stoop from the ground and lowering it asymmetrically on the platform at close (stoop-asymmetric-close).

In the first experimental task, the subject was asked to initially stand in the ready position, then respectively squatting, lift the load, straightening with the load, lowering the load to the determined point on the platform, and finally come to the starting position. A similar process was followed in other experimental tasks. Before the experiment, the subject was given training on the movement to be made.

In a reference study [39], the subject approaches the load by walking, lifts the load of 10 kg in a vertical direction by

crouching and carries the load. The forces acting on the hands of the subject during these movements were calculated using different methods. The results obtained in the reference study [39] are presented according to the directions in the global frame. In order to make a meaningful comparison, in this study, the total force on the hands according to the global frame is recalculated from the force results obtained according to the local references for the right hand frame {34} and for the left hand frame {44},

$$ {}^{0}\boldsymbol{f}_{hands} = {}^{0}_{34}\boldsymbol{R}^{34}\boldsymbol{f}_{34} + {}^{0}_{44}\boldsymbol{R}^{44}\boldsymbol{f}_{44} \tag{18} $$

During these experiments, a metronome was used to ensure that the movements started at approximately the same time.

3. Results and discussion

3.1 *Joint angles*

The angular position changes occurring in the ankle, knee, hip joint, L5/S1, neck, shoulder, elbow and wrist joints of the participant, which are presented as examples in the anthropometric measurements section, are shown as a position-time graph in figures 3, 4 and 5. The results given in figures 3, 4, 5, 6 and 7 were obtained for the squat-symmetric-closed experimental task.

The results of the simulations performed using location data are shown in the figure 6. Figure shows the moments of standing in the starting position (0.3 s), holding the load by squatting (1.1 s), standing with the load (2.3 s), lowering the load on the platform (3.4 s) and returning to the starting position (4.5 s).

3.2 *L5/S1 and upper extremity joint moments*

The net reaction forces and moments occurring in the joints were calculated during the period from taking the load lifted by the subject by squatting to lowering it on the platform in front of him. As mentioned earlier, the forces exerted by the muscles are usually much larger than the net reaction forces. The contribution of the net reaction forces to the compression and shear forces acting on the joint is quite small compared to the muscle forces. The reaction moment is the most important parameter to be verified, as the net reaction moment defines exactly what level of muscle strength is needed to perform a movement [25]. Figure 7 shows the net reaction moments values acting on the wrist, elbow and shoulder joints in the upper extremity group.

Within the scope of this study, participants were asked to perform four different tasks in line with reference studies [25, 37–39]. Figure 8 shows the net reaction moments acting on the L5/S1 joint during the lifting tasks of one of the participants. In figure 8, the 0.3–1.1 s interval is the actions of crouching or bending, the 1.5–2.3 s interval is standing up with the load, the 2.3–2.7 s interval is the actions of standing with the load, the 2.7–3.8 s interval is the actions of leaving the load on the table, and the 2.7–4.5 s interval is the actions of returning to the upright position.

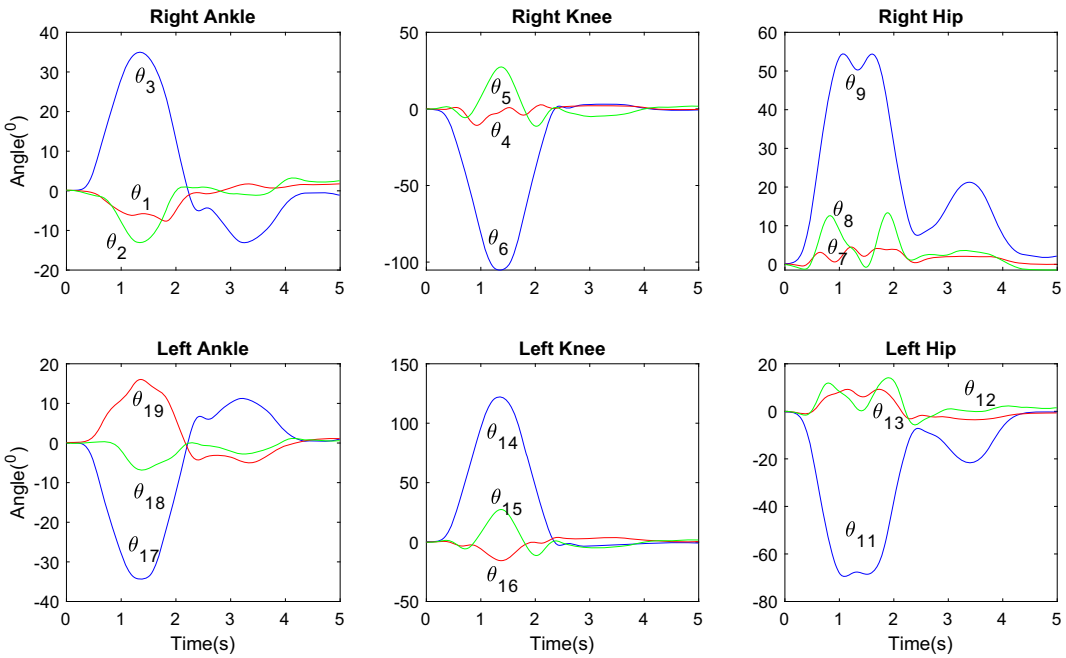

Figure 3. Angular position-time graphs of lower extremity joints.

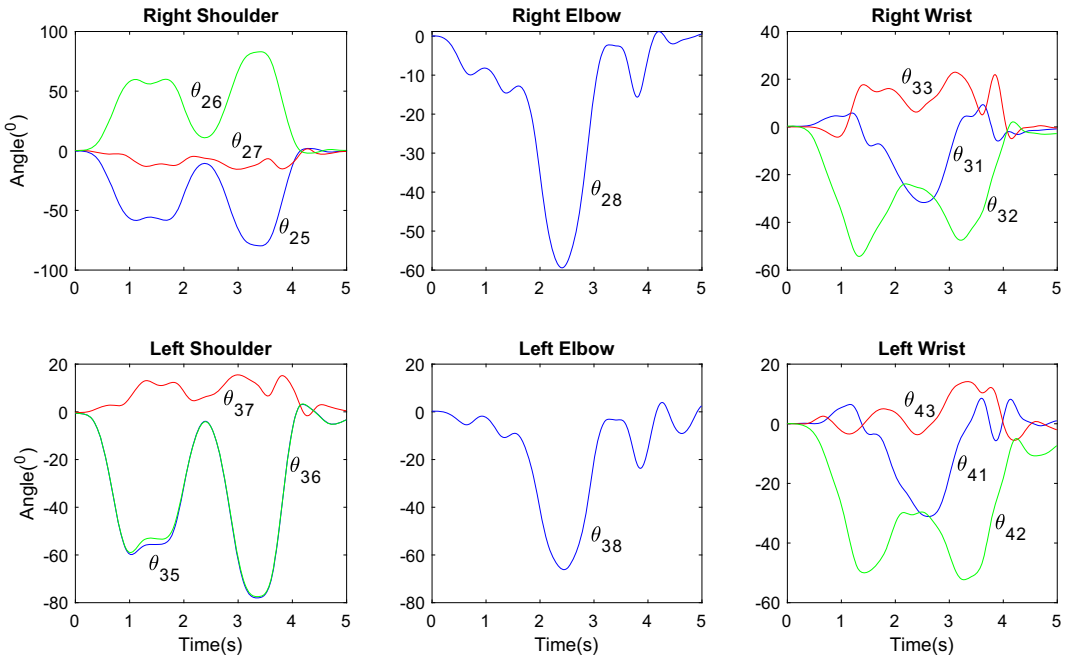

Figure 4. Angular position-time graphs of upper extremity joints.

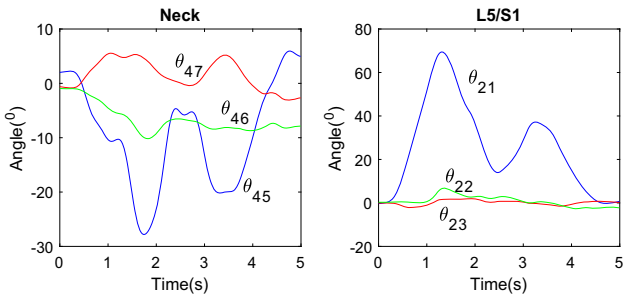

Figure 5. Angular position-time graphs of neck and L5/S1 joints.

Spearman's rank correlation coefficients (rho) values between L5/S1 joint moments for squatting and stooping activities in different lifting tasks are given in table 6. While the results obtained in squatting and stooping activities are completely compatible with each other, they show partial differences. Especially the correlation relationship between squatting and stooping in the extension direction is lower than others. In the activities of standing up with the load, it can be said that a much more stable reaction moment change occurs in standing up from the squatting position compared to stooping. It is observed that there is a significant fluctuation in the reaction moment on the L5/S1 joint, especially in the stooping and asymmetrical lowering activity, as the platform slightly hinders the movement of subject while standing up with the load. During symmetric lowering, the net reaction moments on L5/S1 are concentrated in one axis as expected, whereas in asymmetric lowering they are more in the extension direction but dispersed in all three axes. When the symmetrical lowering is compared among themselves, it is seen that the net reaction moment value in the stoop-symmetric-far graph is quite large compared to the squat-symmetric-close graph. This difference is due to the fact that the load is left at a much farther point in the stoop-symmetric-far action than in the squat-symmetric-close action.

The results of the absolute peak values of the net reaction moments acting on the L5/S1 joint during these lifting tasks are presented in figure 9. Lifting task were tested using a one-way repeated measures analysis of variance (ANOVA). The p-values obtained for different axis by ANOVA analysis for the absolute peak values of the moments given in figure 9; Extension: $p = 0.162$, Lateral Flexion: $p = 0.533$, Twist: $p = 0.014$ (significantly different at $p < 0.05$). From the analysis results, it is seen that there is a significant difference only in the twist moments.

The absolute peak values of the net reaction moments acting on the L5/S1 joint for similar lifting tasks in this study and reference studies [25, 37, 38] and the bilateral t-Test results used to determine the significant difference ($p < 0.05$) are given in table 7. In the reference study [37], some significant differences were observed between the results of four different lifting tasks (free- lowclose, free-low-far, asy-low-close, free-high-close) and four different computational models (buLABmodel, tdLABmodel, tdAMBmodel, buAMBmodel). However, the results obtained with the model proposed in this study are in good agreement with the tdAMBmodel and buAMBmodel computational models in the reference study [37]. Another

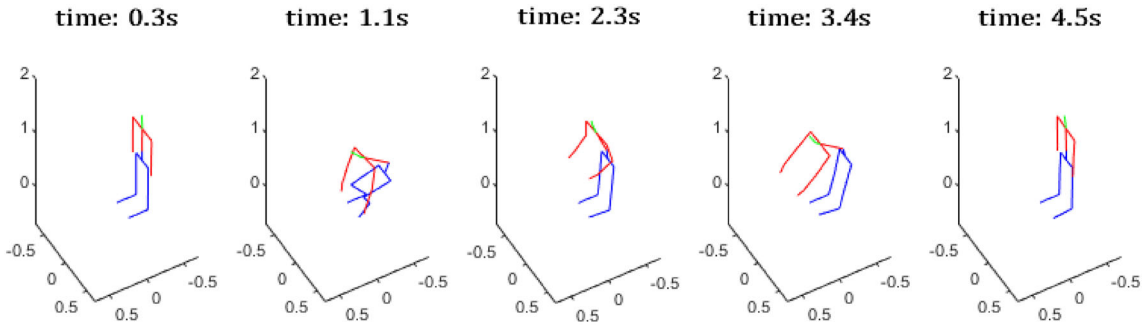

Figure 6. Posture positions of the 3D biomechanical human model at different moments of the squat-symmetric-. experimental task.

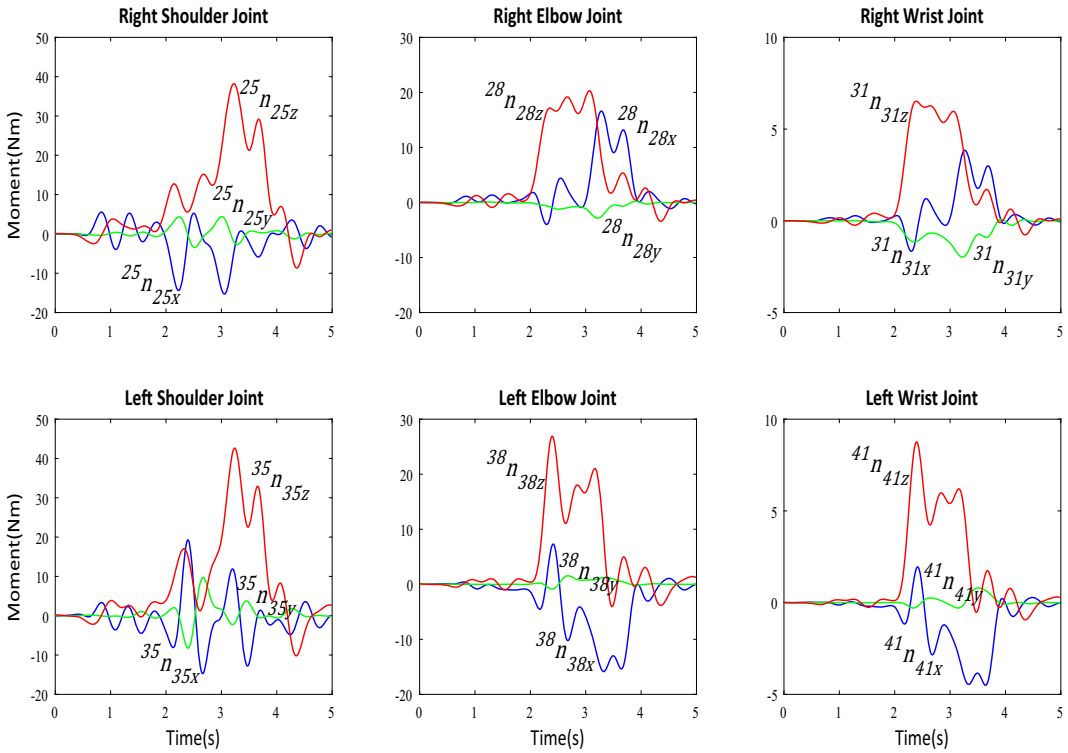

Figure 7. The net reaction moment—time graphs of the joints of the upper extremity.

reference study [38] compared two different lifting tasks and found no significant difference between them except for the twist direction in the squat-symmetric-close task. The comparison with the results of another study [25], which included asymmetric lifting tasks, also showed no significant difference.

3.3 *Hands forces*

The results of this study were obtained for the squat-symmetric-close experimental task and include the process of taking the load from the ground by squatting, lifting it and lowered onto a high platform. The results of the reference study [39] include the processes of free-style lifting and carrying of the load from the ground. Calculation results of hand forces are given in figure 10. In this study, manual lifting starts in approximately 1.8 seconds and lowering is completed in approximately 3.6 seconds. In the reference study [39], manual load lifting starts at approximately 2.8 seconds, and the action of carrying the load continues from approximately 4.6 seconds. It was observed that the results of hand forces were largely similar to the reference study for the relevant time period.

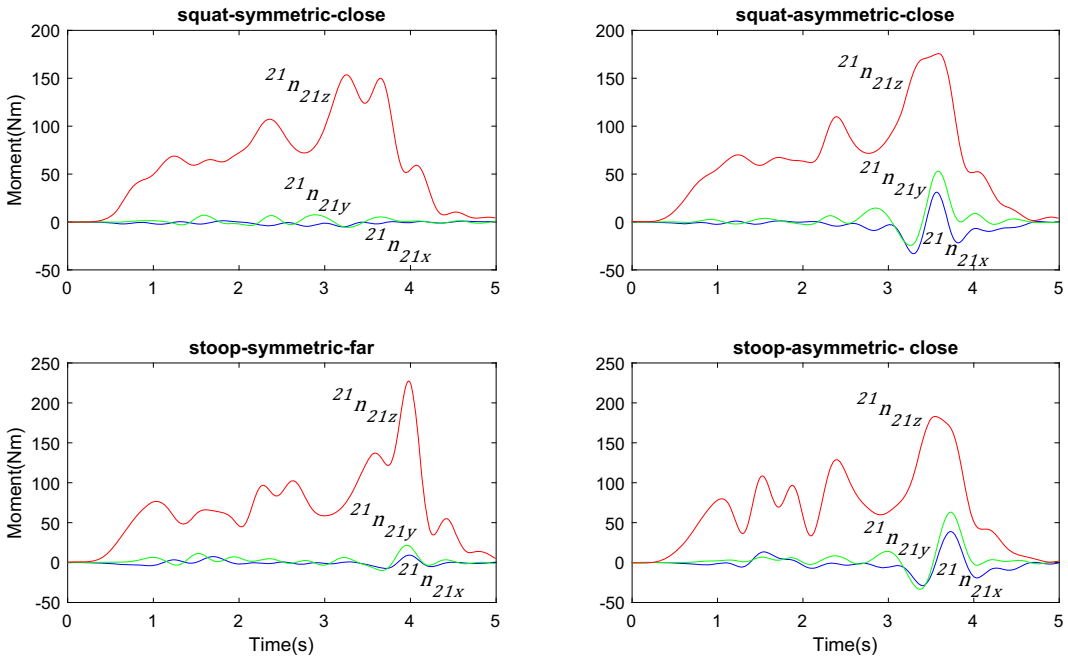

Figure 8. L5/S1 joint squatting/stooping symmetrical and asymmetric the net reaction moment-time graphs.

Table 6. Spearman's rank correlation coefficients (rho) values between the net reaction moments acting on the L5/S1 joint for squatting and stooping activities in different lifting tasks.

Tasks	Extension $^{21}n_{21z}$	Lateral flexion $^{21}n_{21x}$	Twist $^{21}n_{21y}$
Squat-symmetric-close and squat-asymmetric-close	0.729	0.783	1.000
Stoop-symmetric-far and stoop-asymmetric-close	0.878	0.935	0.999
Squat-symmetric-close and stoop-symmetric-far	0.273	0.775	0.995
Squat-asymmetric-close and stoop-asymmetric-close	0.210	0.564	0.997

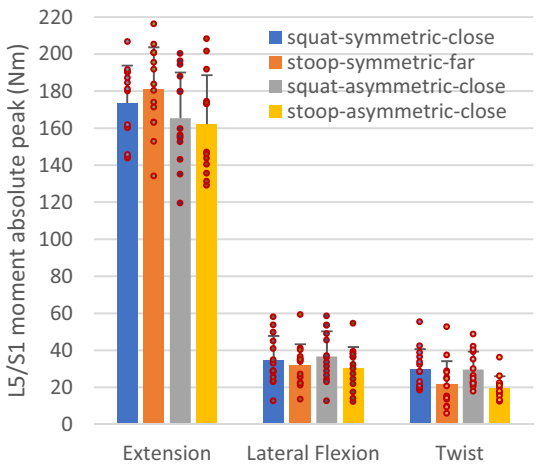

Figure 9. Absolute peak values of the net reaction moments acting on the L5/S1 joint of the participants during different lifting tasks.

3.4 *Limitation*

There are some limitations in this study. Firstly, when both feet are in contact with the ground, the body part from L5/S1 to the feet becomes a parallel mechanism. In this case, in order to calculate the net force and moment values at the hip, knee and ankle joints, a force platform and solution techniques including optimization are needed. However, it is always possible to directly calculate the net reaction forces and moments at the L5/S1, shoulder, elbow and wrist joints with this method, including the case where both feet are in contact with the ground. Secondly, in the application where the proposed model will be used, if an action is to be performed that will cause the feet to lose contact with the ground (such as load carrying), the linear acceleration of the right foot where the reference frame is located should be measured and applied as a boundary condition input to the kinematic equations. Thirdly, during the calculations, it is assumed that the mass of the lifted load is equally distributed to both hands.

Table 7. Absolute peak values and bilateral t-Test results (p-values) of the net reaction moments acting on the L5/S1 joint of similar lifting tasks in this study and reference studies.

	Extension		Lateral flexion		Twist	
	M ± SD	p	M ± SD	p	M ± SD	p
Squat-symmetric-close (This study)	173 ± 20	Control	35 ± 13	Control	32 ± 11	Control
Free-low-close $^{bu}LAB_{model}$ [37]	193 ± 32	0.053	15 ± 6	**< 0.001**	14 ± 7	**< 0.001**
Free-low-close $^{td}LAB_{model}$ [37]	191 ± 33	0.087	14 ± 7	**< 0.001**	16 ± 8	**< 0.001**
Free-low-close $^{td}AMB_{model}$ [37]	177 ± 35	0.709	15 ± 6	**< 0.001**	17 ± 9	**< 0.001**
Free-low-close $^{bu}AMB_{model}$ [37]	158 ± 36	0.178	24 ± 13	**0.028**	18 ± 10	**0.001**
Near reference data [38]	174 ± 75	0.962	44 ± 31	0.334	20 ± 14	**0.025**
Stoop-symmetric-far (This study)	181 ± 23	Control	32 ± 11	Control	21 ± 13	Control
Free-low-far $^{bu}LAB_{model}$ [37]	213 ± 35	**0.007**	15 ± 6	**< 0.001**	19 ± 8	0.611
Free-low-far $^{td}LAB_{model}$ [37]	215 ± 39	**0.008**	14 ± 7	**< 0.001**	20 ± 11	0.821
Free-low-far $^{td}AMB_{model}$ [37]	204 ± 47	0.108	15 ± 7	**< 0.001**	23 ± 11	0.652
Free-low-far $^{bu}AMB_{model}$ [37]	177 ± 44	0.763	24 ± 14	0.096	22 ± 9	0.806
Far reference data [38]	185 ± 71	0.844	40 ± 18	0.183	19 ± 12	0.697
Squat-asymmetric-close (This study)	165 ± 25	Control	37 ± 14	Control	30 ± 10	Control
Asy-low-close $^{bu}LAB_{model}$ [37]	177 ± 44	0.376	42 ± 21	0.456	22 ± 7	**0.016**
Asy-low-close $^{td}LAB_{model}$ [37]	183 ± 46	0.203	38 ± 20	0.877	22 ± 7	**0.016**
Asy-low-close $^{td}AMB_{model}$ [37]	172 ± 42	0.591	39 ± 20	0.757	27 ± 12	0.467
Asy-low-close $^{bu}AMB_{model}$ [37]	167 ± 48	0.890	44 ± 22	0.316	27 ± 14	0.511
Bottom-up [25]	174 ± 43	0.548	44 ± 22	0.383	32 ± 21	0.768
Top-down [25]	191 ± 50	0.124	55 ± 29	0.067	34 ± 18	0.516
Stoop -asymmetric-close (This study)	162 ± 27	Control	30 ± 12	Control	20 ± 6	Control
Asy-low-close $^{bu}LAB_{model}$ [37]	177 ± 44	0.279	42 ± 21	0.070	22 ± 7	0.412
Asy-low-close $^{td}LAB_{model}$ [37]	183 ± 46	0.146	38 ± 20	0.203	22 ± 7	0.412
Asy-low-close $^{td}AMB_{model}$ [37]	172 ± 42	0.452	39 ± 20	0.154	27 ± 12	0.058
Asy-low-close $^{bu}AMB_{model}$ [37]	167 ± 48	0.733	44 ± 22	**0.043**	27 ± 14	0.094

Bold p-values are significantly different at $p < 0.05$.

M Mean; *SD* Standard deviation.

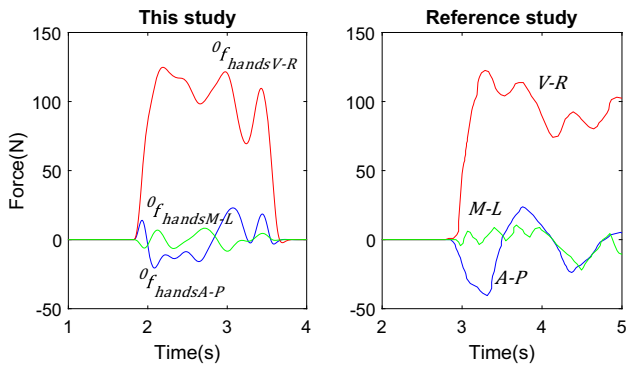

Figure 10. Hand forces in each axis (A-P = anteroposterior; M-L = mediolateral; V-R = vertical) for a volunteer participant in this study and for any participant of the reference study [39].

4. Conclusion

In this study, it is aimed to develop a method that can calculate the net reaction forces and moments acting on the L5/S1 and upper extremity joints by using only kinematic measurement inputs, without the need for force measurement from the points where the feet contact the ground. Joint motion inputs can be obtained using any motion capture method (optical motion capture, inertial motion capture or, etc.). In the application where the proposed model will be used, if an action is to be performed that will cause the feet to lose contact with the ground (such as load handling), the linear acceleration of the right foot where the reference frame is located should be measured and applied as a boundary condition input to the kinematic equations. The results obtained from the experimental study involving manual load lifting and dropping activities using this method were found to be consistent with the results obtained from peer experimental studies carried out in the literature under similar conditions. It is predicted that this model can be used for the analysis of human movement behavior in areas such as ergonomics studies, determination of movement disorders, orthosis/prosthesis designs and sports activities.

Acknowledgements

The authors acknowledge Dr Bilal Usanmaz for his assistance in data acquisition and processing.

Funding This study was supported by Ataturk University Scientific Research Projects (BAP) Coordination Unit (Project no: FOA-2018-6529).

Declarations

Conflict of interest The authors declare that they have no known competing financial interests or personal relationships that could have appeared to influence the work reported in this paper.

References

[1] Barman S, Xiang Y, Rakshit R and Yang J 2022 Joint fatigue-based optimal posture prediction for maximizing endurance time in box carrying task. *Multibody Sys. Dyn.* 55(3): 323–339

[2] Chang C-C, McGorry R W, Lin J, Xu X and Hsiang S M 2010 Prediction accuracy in estimating joint angle trajectories using a video posture coding method for sagittal lifting tasks. *Ergonomics* 53: 1039–1047

[3] Gündogdu Ö, Anderson K S and Parnianpour M 2005 Simulation of manual materials handling: Biomechanial assessment under different lifting conditions. *Technol. Health Care* 13: 57–66

[4] Hsiang S M and Ayoub M M 1994 Development of methodology in biomechanical simulation of manual lifting. *Int. J. Ind. Ergon.* 13: 271–288

[5] Khalaf K A, Parnianpour M, Sparto P J and Barin K 1999 Determination of the effect of lift characteristics on dynamic performance profiles during manual materials handling tasks. *Ergonomics* 42: 126–145

[6] Lo J, Huang G and Metaxas D 2002 Human motion planning based on recursive dynamics and optimal control techniques. *Multibody Sys. Dyn.* 8: 433–458

[7] Song J, Qu X and Chen C-H 2016 Simulation of lifting motions using a novel multi-objective optimization approach. *Int. J. Ind. Ergon.* 53: 37–47

[8] Usanmaz B and Gündoğdu Ö 2014 Neuro-fuzzy modeling of manual materials handling. *Ordu Univ. J. Sci. Technol.* 4: 36–45

[9] Xiang Y, Zaman R, Rakshit R and Yang J 2019 Subject-specific strength percentile determination for two-dimensional symmetric lifting considering dynamic joint strength. *Multibody Sys. Dyn.* 46: 63–76

[10] Xiang Y, Arora J S, Rahmatalla S, Marler T, Bhatt R and Abdel-Malek K 2010 Human lifting simulation using a multi-objective optimization approach. *Multibody Sys. Dyn.* 23: 431–451

[11] Yanıkören M, Yılmaz S, Usanmaz B, Tezgel S, Yazar M and Gündoğdu Ö 2020 Determination of the forces and torques acting on the upper limb joints with dynamic model using wearable motion sensors. *J. Inst. Sc. Technol.* 10: 2850–2859

[12] Ding Z 2013 Manual assembly modelling and simulation for ergonomics analysis, PhD Thesis, University of Liverpool, UK

[13] Kim J H, Abdel-Malek K, Yang J, Marler T and Nebel K 2005 Lifting posture analysis in material handling using virtual humans. In: *ASME International Mechanical Engineering Congress and Exposition*, pp. 1445–1453

[14] Wu Z, Zhao H, Zheng G, Wu S, Xu R and Xie Y 2021 Structural self-similarity framework for virtual human's whole posture generation. *Arabian J. Sci. Eng.* 46: 8617–8628

[15] Chaffin D B 1969 A computerized biomechanical model—development of and use in studying gross body actions. *J. Biomech.* 2: 429–441

[16] Morris J M, Lucas D B and Bresler B 1961 Role of the trunk in stability of the spine. *JBJS* 43: 327–351

[17] Ayoub M M 1992 Problems and solutions in manual materials handling: the state of the art. *Ergonomics* 35: 713–728

[18] Chang C-C, Hsiang S, Dempsey P G and McGorry R W 2003 A computerized video coding system for biomechanical analysis of lifting tasks. *Int. J. Ind. Ergon.* 32: 239–250

[19] De Looze M P, Kingma I, Bussmann J B J and Toussaint H M 1992 Validation of a dynamic linked segment model to calculate joint moments in lifting. *Clin. Biomech.* 7: 161–169

[20] Marras W S and Davis K G 1998 Spine loading during asymmetric lifting using one versus two hands. *Ergonomics* 41: 817–834

[21] Kim H J, Wang Q, Rahmatalla S, Swan C C, Arora J S, Abdel-Malek K and Assouline J G 2008 Dynamic motion planning of 3D human locomotion using gradient-based optimization. *J. Biomech. Eng.* 130(3): 031002

[22] Abdel-Malek K, Yu W, Mi Z, Tanbour E and Jaber M 2001 Posture prediction versus inverse kinematics. In: *International Design Engineering Technical Conferences and Computers and Information in Engineering Conference (ASME),* pp. 37–45

[23] Amca A M, Harbili E and Aritan S 2010 Development of mechanical model of olympic snatch for biomechanical analysis. *Hacettepe Journal of Sport Sciences* 21: 21–29

[24] Asfour S S, Waly S M and Fahmy M W 1991 A 2-dimensional computerized biomechanical model. *Comput. Ind. Eng.* 21: 601–605

[25] Kingma I, de Looze M P, Toussaint H M, Klijnsma H G and Bruijnen T B M 1996 Validation of a full body 3-D dynamic linked segment model. *Hum. Mov. Sci.* 15: 833–860

[26] Serbest K, Çilli M and Eldoğan O 2013 Oturulan yerden kalkma hareketinin analizi için mekanik model geliştirilmesi. *Sakarya University Journal of Science* 17: 189–193

[27] Waters T R and Garg A 2010 Two-dimensional biomechanical model for estimating strength of youth and adolescents for manual material handling tasks. *Appl. Ergon.* 41: 1–7

[28] Winter D A 2009 Biomechanics and motor control of human movement. John Wiley & Sons

[29] Dempsey P G 2003 A survey of lifting and lowering tasks. *Int. J. Ind. Ergon.* 31: 11–16

[30] Lorenzo Munar and Maurizio Curtarelli 2019 Work-related musculoskeletal disorders: prevalence, costs and demographics in the EU, European Agency for Safety and Health at Work

[31] McGuinness S 2022 Annual review of workplace injuries, illnesses and fatalities 2020–2021, Health and Safety Authority

[32] Chaffin D B and Erig M 1991 Three-dimensional biomechanical static strength prediction model sensitivity to postural and anthropometric inaccuracies. *IIE Trans.* 23(3): 215–227
[33] Zaman R, Xiang Y, Rakshit R and Yang J 2022 Hybrid predictive model for lifting by integrating skeletal motion prediction with an OpenSim musculoskeletal model. *IEEE Trans. Biomed. Eng.* 69(3): 1111–1122
[34] Nimbarte A D, Sun Y, Jaridi M and Hsiao H 2013 Biomechanical loading of the shoulder complex and lumbosacral joints during dynamic cart pushing task. *Appl. Ergon.* 44: 841–849
[35] Parida R and Ray P K 2015 Biomechanical modelling of manual material handling tasks: a comprehensive review. *Procedia Manuf.* 3: 4598–4605
[36] Akhavanfar M, Uchida T K, Clouthier A L and Graham R B 2022 Sharing the load: modeling loads in OpenSim to simulate two-handed lifting. *Multibody Sys. Dyn.* 54: 213–234
[37] Faber G S, Kingma I, Chang C C, Dennerlein J T and van Dieën J H 2020 Validation of a wearable system for 3D ambulatory L5/S1 moment assessment during manual lifting using instrumented shoes and an inertial sensor suit. *J. Biomech.* 102: 109671
[38] Xu X, Chang C-C, Faber G S, Kingma I and Dennerlein J T 2012 Estimation of 3-D peak L5/S1 joint moment during asymmetric lifting tasks with cubic spline interpolation of segment Euler angles. *Appl. Ergon.* 43: 115–120
[39] Faber G S, Koopman A S, Kingma I, Chang C C, Dennerlein J T and van Dieën J H 2018 Continuous ambulatory hand force monitoring during manual materials handling using instrumented force shoes and an inertial motion capture suit. *J. Biomech.* 70: 235–241
[40] Larivière C and Gagnon D 1999 The L5/S1 joint moment sensitivity to measurement errors in dynamic 3D multisegment lifting models. *Hum. Mov. Sci.* 18: 573–587
[41] Denavit J and Hartenberg R S 1955 A kinematic notation for lower-pair mechanisms based on matrices. *J. Appl. Mech.* 22(2): 215–221
[42] Craig J J 2005 Introduction to robotics: mechanics and control. 3rd edn. Pearson Education
[43] Ahmed D B and Metzger K 2018 Wearable-based pedestrian inertial navigation with constraints based on biomechanical models. In: *IEEE/ION Position, Location and Navigation Symposium,* pp. 118–123
[44] Arisumi H, Miossec S, Chardonnet J-R and Yokoi K 2008 Dynamic lifting by whole body motion of humanoid robots. In: *IEEE/RSJ International Conference on Intelligent Robots and Systems,* pp. 668–675
[45] Yang J J and Kim J H 2010 Static joint torque determination of a human model for standing and seating tasks considering balance. *J. Mech. Rob.* 2: 031005
[46] Plamondon A, Gagnon M and Desjardins P 1996 Validation of two 3-D segment models to calculate the net reaction forces and moments at the L5/S1 joint in lifting. *Clin. Biomech.* 11(2): 101–110
[47] Faber G S, Kingma I, Kuijer P P F M, van der Molen H F, Hoozemans M J M, Frings-Dresen M H W and van Dieën J H 2009 Working height, block mass and one- vs. two-handed block handling: the contribution to low back and shoulder loading during masonry work. *Ergonomics* 52: 1104–1118
[48] Plamondon A, Larivière C, Denis D, Mecheri H and Nastasia I 2017 Difference between male and female workers lifting the same relative load when palletizing boxes. *Appl. Ergon.* 60: 93–102
[49] Faber G S, Chang C C, Kingma I, Dennerlein J T and van Dieën J H 2016 Estimating 3D L5/S1 moments and ground reaction forces during trunk bending using a full-body ambulatory inertial motion capture system. *J. Biomech.* 49: 904–912
[50] Kim S and Nussbaum M A 2013 Performance evaluation of a wearable inertial motion capture system for capturing physical exposures during manual material handling tasks. *Ergonomics* 56: 314–326
[51] Muller A, Pontonnier C, Robert-Lachaine X, Dumont G and Plamondon A 2020 Motion-based prediction of external forces and moments and back loading during manual material handling tasks. *Appl. Ergon.* 82: 102935
[52] Roetenberg D, Luinge H and Slycke P 2013 Xsens MVN: Full 6DOF human motion tracking using miniature inertial sensors. *Xsens Technologies* 1–9
[53] Yu B, Gabriel D, Noble L and An K-N 1999 Estimate of the optimum cutoff frequency for the Butterworth low-pass digital filter. *J. Appl. Biomech,* 15: 318–329
[54] Robertson D G E and Dowling J J 2003 Design and responses of Butterworth and critically damped digital filters. *J. Electromyogr. Kinesiol.* 13: 569–573
[55] Robinette K M, Blackwell S, Daanen H, Boehmer M, Fleming S, Brill T, Hoeferlin D and Burnsides D 2002 Civilian american and european surface anthropometry resource (caesar) final report, Volume I: Summary, United States Air Force Research Laboratory, SAE International
[56] Gillette J C 1999 *A three-dimensional, dynamic model of the human body for lifting motions*, PhD Thesis, Iowa State University, USA